Catalysis Science & Technology

This article can be cited before page numbers have been issued, to do this please use: K. Motokura, K. Saitoh, H. Noda, W. Chun, A. Miyaji, S. Yamaguchi and T. Baba, *Catal. Sci. Technol.*, 2016, DOI: 10.1039/C6CY00593D.

ROYAL SOCIETY OF CHEMISTRY

www.rsc.org/catalysis

View Article Online
DOI: 10.1039/C6CY00593D

Pd-Bisphosphine Complex and Organic Functionalities Immobilized on the Same SiO_2 Surface: Detailed Characterization and Its Use as an Efficient Catalyst for Allylation

Ken Motokura,[1] Koki Saitoh,[1] Hiroto Noda,[1] Wang-Jae Chun,[2] Akimitsu Miyaji,[1] Sho Yamaguchi,[1] Toshihide Baba*,[1]

[1] *Department of Environmental Chemistry and Engineering, Tokyo Institute of Technology, 4259 Nagatsuta-cho, Midori-ku, Yokohama, 226-8502, Japan*
E-mail: tbaba@chemenv.titech.ac.jp
[2] *Graduate School of Arts and Sciences, International Christian University, Mitaka, Tokyo, 181-8585, Japan*

ABSTRACT:

Pd-bisphosphine complex and several organic functionalities were immobilized on the same SiO_2 surface. The samples thus prepared were characterized by solid-state NMR, XPS, and XAFS. Based on the curve-fitting analysis of Pd K-edge EXAFS spectra, both the local environment of the immobilized Pd complexes and interactions with the co-immobilized organic functions were discussed. The SiO_2-supported Pd-bisphosphine complex and DABCO exhibited excellent catalytic performance for the allylation of various nucleophiles: a TON of up to 106000 was obtained. Both the catalyst activation pathway and reaction mechanism were also discussed on the basis of the structure of the used catalyst samples.

KEYWORDS: *synergistic catalysis, palladium, organic base, bisphosphine, allylation*

View Article Online
DOI: 10.1039/C6CY00593D

Introduction

The palladium-catalyzed allylation of nucleophiles is one of the most efficient protocols for constructing C-C bonds and introducing highly reactive allyl groups.[1] Various homogeneous and heterogeneous palladium catalysts for allylation have been reported.[2,3] Scheme 1 shows the previously reported Pd-catalyzed allylation systems exhibiting very high turnover numbers (TONs). Uozumi and co-workers have investigated the allylation of aromatic nucleophiles using both homogeneous[2a] and heterogeneous[3a] catalysts with excellent TONs of 500 000 000 and 1250 000, respectively. Moreover, Santelli and co-workers have reported a TON of 9800 000 for the allylation of alkyl nucleophiles, such as active methylenes, using a homogeneous Pd-Tedicyp catalyst in the presence of stoichiometric amount of NaH (Scheme 1).[2b] The pre-activation of the alkyl C-H bond significantly enhances the reactivity of the nucleophile; however, in this case, the formation of stoichiometric salt wastes cannot be avoided. On the other hand, TONs of up to 2000 have been reported for Pd catalyst systems using alkyl nucleophiles without pre-activation.[2,3]

For overcoming this problem, the concept, involving the synergistic activation of both the allylating reagent and nucleophile by Pd species and catalytic amount of base, respectively, should be effective.[4] This concept of synergistic activation has been demonstrated by Muzart and co-workers in 1987 with the use of a heterogeneous catalysis system.[3c] On the other hand, our group has also been continuously developing a bifunctional catalytic surface composed of Pd- and an organic base, which enables the synergistic activation of both allylating reagents and nucleophiles.[5,6] Especially, a Pd-bisphosphine complex immobilized on SiO_2 surface with 1,4-diazabicyclo[2.2.2]octane (DABCO) functionality was found to be a potentially

View Article Online
DOI: 10.1039/C6CY00593D

highly active catalyst.[5c] The formation of stoichiometric waste can be avoided by the use of a co-immobilized amine base, which serves as a catalyst for activating the nucleophile. In addition, the close proximity of the Pd complex and organic base on the same solid surface induces efficient bond formation between the activated substrate molecules.

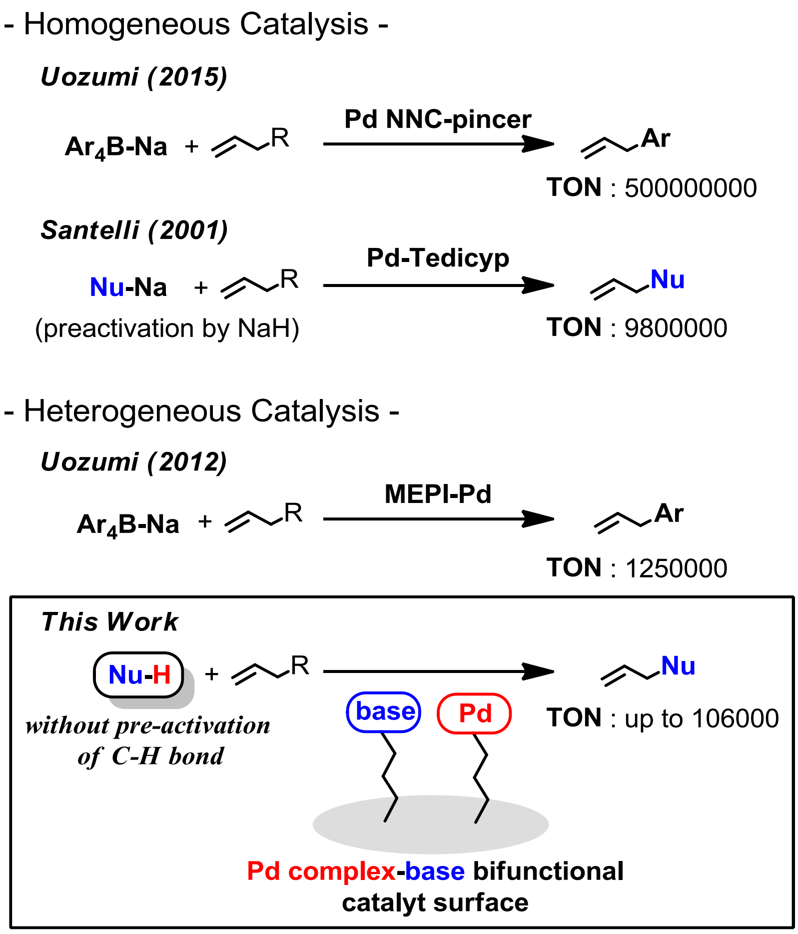

Scheme 1. Homogeneous and heterogeneous Pd-catalyzed allylation reaction systems exhibiting high turnover numbers. Nu: alkyl carbon nucleophile, R: leaving group such as methyl carbonate.

In this paper, we fully investigate the synergistic catalysis between a Pd-bisphosphine complex and organic functions immobilized on the same SiO_2 surface, including the

View Article Online
DOI: 10.1039/C6CY00593D

detailed catalyst structure, interaction between the Pd complex and organic functions, and substrate scope as well as mechanism of allylation. In the case of a catalyst with DABCO functionality, the highest TON based on Pd of up to 106000 was achieved without the pre-activation of nucleophile (Scheme 1, *this study*).

Results and Discussion

Preparation of SiO_2-supported Pd Complexes

SiO_2-supported Pd-bisphosphine complex catalysts were prepared by a simple silane-coupling reaction. As shown in Scheme 2, a Pd complex precursor (PP-Pd) was prepared from a bisphosphine ligand having a triethoxysilane group and $[PdCl(\eta^3\text{-allyl})]_2$.[5c] ^1H, ^{13}C, ^{31}P, ^1H-^1H COSY, ^1H-^{13}C HSQC NMR, and HRMAS analyses clearly indicate the formation of the PP-Pd complex structure (Supporting Information, Figure S1 and S2). The silane-coupling reaction between SiO_2 (Aerosil300) and PP-Pd afforded the SiO_2-supported Pd-bisphosphine complex (SiO_2/PP-Pd) (Scheme 3a).[5c,7] Other supported catalysts having organic functional groups on the same surface were prepared from pre-functionalized SiO_2 and PP-Pd. For DABCO-immobilized SiO_2, SiO_2 was treated with chloropropyltrimethoxysilane to afford SiO_2/Cl, followed by quaternization between SiO_2/Cl and DABCO, affording SiO_2/DABCO (Scheme S1, Supporting Information).[5c] SiO_2 with methyl and *n*-hexyl groups (SiO_2/Me and SiO_2/Hex, respectively) were also prepared by the silane-coupling reaction (Scheme 4). Pre-functionalized SiO_2 (SiO_2/R) was treated with PP-Pd to afford the corresponding SiO_2-supported functional group (R) and Pd complex (SiO_2/R/PP-Pd), as shown in Scheme 3b-d.

View Article Online
DOI: 10.1039/C6CY00593D

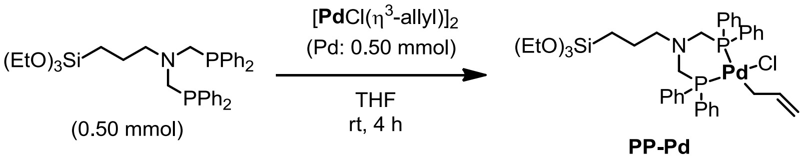

Scheme 2. Preparation of Pd-bisphosphine complex (PP-Pd).

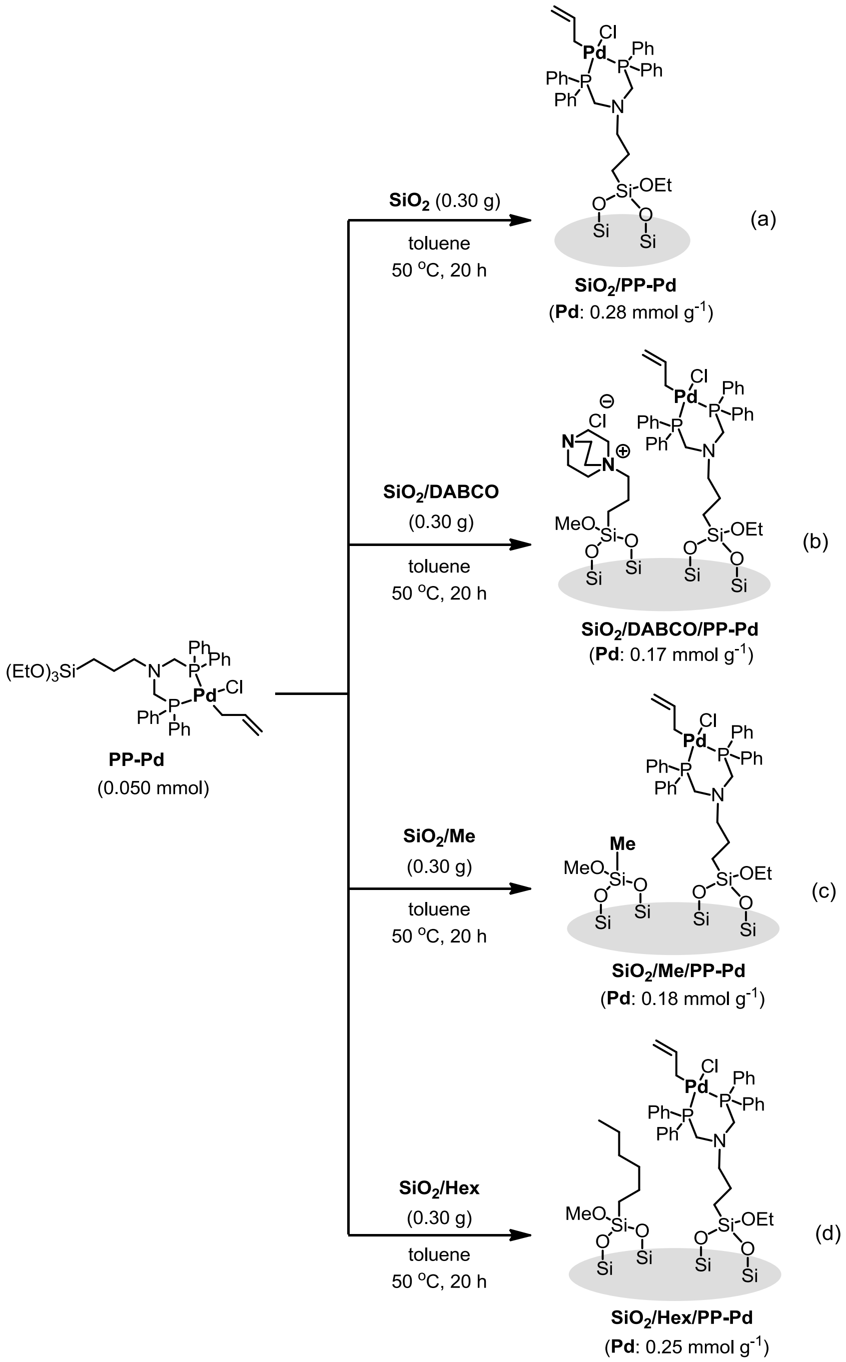

Scheme 3. Preparation of SiO_2/DABCO/PP-Pd, SiO_2/PP-Pd, SiO_2/Me/PP-Pd, and SiO_2/Hex/PP-Pd

View Article Online
DOI: 10.1039/C6CY00593D

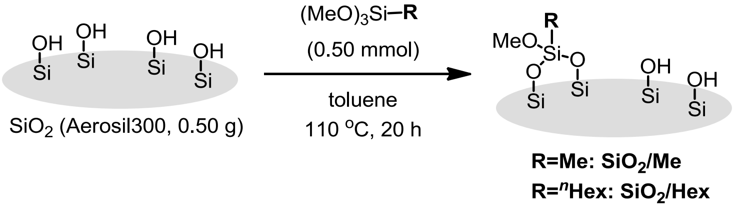

Scheme 4. Preparation of SiO_2-supported organic functions (SiO_2/Me and SiO_2/Hex).

Characterization of SiO_2-supported Pd Complexes

Table 1 summarizes the results obtained from the elemental analysis of the prepared samples. For SiO_2/DABCO, the nitrogen:chlorine ratio was *ca.* 2, indicative of the formation of the quaternized DABCO structure.[5c] ^{13}C CP/MAS NMR analysis was employed for confirming the quantitative formation of quaternized DABCO from the chloropropyl functionality of SiO_2/Cl (Figure S3, Supporting Information).[5c] Similar nitrogen, chlorine, and palladium contents were obtained for SiO_2/PP-Pd, SiO_2/Me/PP-Pd, and SiO_2/Hex/PP-Pd, implying that the PP-Pd complex structure (N:Cl:Pd=1:1:1) on the SiO_2 surface is maintained. As compared with that in SiO_2/PP-Pd, the nitrogen and chlorine content in SiO_2/DABCO/PP-Pd increased because of the immobilization of quaternized DABCO.

The coordination structure and carbon skeleton of the immobilized functions were determined by solid-state ^{31}P and ^{13}C MAS NMR analysis, respectively. A strong signal was observed at around 0 ppm in the ^{31}P MAS NMR spectra of all supported Pd-bisphosphine complex samples, implying that the Pd-bisphosphine complex structure of PP-Pd is maintained (solution-state ^{31}P NMR: 3 ppm) (Figure S4, Supporting Information). Figure 1 shows the results obtained from the ^{13}C NMR spectra. The ^{13}C NMR signals of the main carbon skeleton (*a*-*e* and Ph) of PP-Pd (a) were

View Article Online
DOI: 10.1039/C6CY00593D

observed in SiO_2/PP-Pd (b). These signals were also detected in other SiO_2-supported Pd complexes with other organic functions (SiO_2/R/PP-Pd) (c-e). In addition, the signals derived from the co-immobilized organic functions were observed: for example, in SiO_2/DABCO/PP-Pd (e), the signals of carbons next to the nitrogen atoms of quaternized DABCO were detected at 46, 53, and 66 ppm (blue symbols).[5c]

Table 2 shows the XPS signals of SiO_2-supported Pd complexes. Figure 2 shows the XPS spectra of Pd_{3d}, N_{1s}, and Cl_{2p}. As shown in Table 2 and Figure 2(A), the $Pd_{3d5/2}$ signals of all samples were observed at 337.2-337.5 eV, corresponding to the Pd(II) species with the phosphine ligand.[7] The signals of the P_{2p} region were observed at 131.1-131.6 eV, also corresponding to the Pd-bisphosphine complex structure (Table 2) [7]. For SiO_2/DABCO/PP-Pd, two N_{1s} signals were detected (399.6 and 402 eV, respectively), while for other SiO_2-supported Pd samples, only one signal was observed (Table 2, Figure 2(B)), indicating the presence of tertiary and quaternized amine groups in SiO_2/DABCO/PP-Pd.[5c,8] The 1:2 atomic ratio of Pd and P was also detected by XPS analysis.

For determining the detailed local structure of immobilized Pd complexes, Pd K-edge XAFS analysis was conducted.[9] XANES, EXAFS, and the Fourier transform (FT) of k^3-weighted Pd K-edge EXAFS spectra (Figures S5-S7, Supporting Information) of PP-Pd precursor, SiO_2/PP-Pd, and SiO_2/R/PP-Pd were almost identical.

Table 3 summarizes the curve-fitting results of EXAFS spectra. For SiO_2/DABCO/PP-Pd, the coordination number (N) and bond length (r) were evaluated as 3.0 ± 0.5 and 2.26 ± 0.01 Å, respectively. This bond length was similar to those of the Pd-P/Cl bonds in Pd(II)$Cl_2(PPh_3)_2$ (average values: 2.32 Å).[10] These results clearly support the proposed structure of the Pd complex on the SiO_2 surface: two Pd-P and one

View Article Online
DOI: 10.1039/C6CY00593D

Pd-Cl bonds. As shown in Table 3, other fresh SiO_2-supported Pd complexes exhibited similar N (2.6-2.9) and r values (2.26-2.27 Å), and these values were almost identical to those of the PP-Pd precursor.

The above EXAFS analysis has revealed the maintenance of the local coordination atoms in the first shell of all the Pd complexes immobilized on the SiO_2 surface both with and without the co-immobilized organic functions. The EXAFS results have enlightened that no specific change is observed in the local structure of the immobilized Pd complexes on the SiO_2 surface both with and without co-immobilizers. Noteworthy, however, is the clear changes in the Debye-Waller factors ($\Delta\sigma^2$). As shown in Table 3, the $\Delta\sigma^2$ values of the SiO_2-supported samples were clearly affected by the co-immobilized organic functions. Figure 3 (○) shows the dependence of the $\Delta\sigma^2$ value on the size of the co-immobilized functions on the same SiO_2 surface. The $\Delta\sigma^2$ value increased with the increasing size of the co-immobilized molecule. As the Debye-Waller factor is complementary with the coordination number (N), the $\Delta\sigma^2$ value was simulated with a fixed coordination number N=3 (Figure 3; ▲): similar phenomena were also observed. The Debye-Waller factor comprises contributions from both static and dynamic disorder: $\sigma^2=\sigma_{\mathrm{static}}{}^2+\sigma_{\mathrm{dynamic}}{}^2$. As shown in Table 3, the bond length (r) of the Pd complex immobilized on the SiO_2 surface was almost same, indicating $\sigma_{\mathrm{dynamic}}{}^2$, which should be related to $\nu_{\mathrm{Pd\text{-}P/Cl}}$, does not change by the size of the co-immobilized organic functions.[11] In conclusion, the σ_{static} value can be expected to increase by the static disorder of the Pd complex immobilized on the SiO_2 surface by the steric effect attributed to the co-immobilized organic functions. Figure 4 shows the schematic of the order of the steric effect. The Pd complex and co-immobilized organic functions, especially DABCO, existed in close proximity, suggesting their cooperation for a single

View Article Online
DOI: 10.1039/C6CY00593D

catalytic transformation.

Allylation Catalyzed by SiO_2-supported Pd Complexes

The prepared SiO_2-supported Pd complex were used for the allylation between ethyl acetoacetate and allylmethylcarbonate. Table 4 summarizes the results. The reaction bewteen 0.5 mmol of ethyl acetoacetate and 2.5 equivalent of allylmethylcarbonate using 3.0 μmol of Pd in SiO_2/DABCO/PP-Pd afforded allylated products in a total yield of 99% with a TON of 300 (entry 1). With the use of the supported catalyst without DABCO under the same reaction conditions, the TON decreased to 230 (entry 2). With the use of other organic functions, such as methyl and hexyl groups (entries 3 and 4, respectively), the product yield and TON did not increase as compared with those observed with the use of SiO_2/PP-Pd. These results clearly indicate that only DABCO can enhance the allylation reaction. As shown in the above section, the Debye-Waller factor ($\Delta\sigma^2$) of SiO_2/DABCO/PP-Pd and SiO_2/Hex/PP-Pd were almost the same, while the catalytic activity (TON) of SiO_2/DABCO/PP-Pd was significantly higher than that of SiO_2/Hex/PP-Pd. This result indicates that the static disorder of the Pd complex scarcely affects the catalytic activity.

The homogeneous Pd precursor (PP-Pd) exhibited catalytic activity similar to that exhibited by the supported SiO_2/PP-Pd catalyst (entry 5), indicating the catalytic activity of the PP-Pd complex is maintained after the immobilization on the SiO_2 surface. On the other hand, the addition of DABCO to the homogeneous PP-Pd catalyst system did not enhance its catalytic activity (entry 6). Interestingly, the co-immobilization of both PP-Pd and DABCO function on the SiO_2 surface is necessary for enhancing the catalytic activity.

View Article Online
DOI: 10.1039/C6CY00593D

As the SiO_2/DABCO/PP-Pd catalyst exhibited the highest activity for the allylation reaction, the substrate scope was examined using this SiO_2/DABCO/PP-Pd catalyst under solvent-free conditions. Table 5 summarizes the results. Surprisingly, the reaction of acetylacetone using 0.002 mol% of Pd in SiO_2/DABCO/PP-Pd afforded the corresponding allylated products in a total yield of 90%, with a TON of 106000 (entry 1). To the best of our knowledge, this TON value is more than two orders higher than those of previously reported catalyst systems without the pre-activation of the alkyl C-H bond of nucleophiles. Other nucleophiles, such as nitrile, diketone, ketoester, and even diester, exhibited high reactivity, affording the corresponding diallylated prodcuts in good to quantitative yields with a TON of greater than 11000 (entries 3, 4, 6, and 7, respectively) except in the case of a steric bulk substrate (entry 5). For a ketoester with one α-proton, mono allyaltion selectively proceeded, affording the corresponding product in 98%, with a TON of 11700 (entry 6). Phenol was also found to be a reactive nucleophile in this catalyst system (entry 8). In all cases, the reaction smoothly proceeded in the presence of a very small amount of K_2CO_3.

To check the heterogeneous catalysis of the active SiO_2/DABCO/PP-Pd, a hot filtration test was conducted. After the removal of the solid catalyst at around a TON of 200, further allylation in the filtrate hardly occurred, suggesting that the reaction proceeds on the solid surface. Regarding catalyst durability, after the completion of the reaction of ethyl acetoacetate using SiO_2/DABCO/PP-Pd, new substrates were added to the reaction mixture. A further reaction proceeded to give almost quantitative yield of the allylated products for at least 6 cycles.[5c]

View Article Online
DOI: 10.1039/C6CY00593D

Catalyst Activation Pathway and Catalytic Reaction Mechanism

Characterization results indicated that the Pd species in the SiO_2-supported Pd-bisphosphine complexes is divalent with respect to chloride and the η^1-allyl anion [PP-Pd(η^1-allyl)Cl]. Figure 5 shows the Pd K-edge XANES spectra of fresh SiO_2/DABCO/PP-Pd, SiO_2/DABCO/PP-Pd-used, and several reference samples. The XANES position of SiO_2/DABCO/PP-Pd barely changed after the catalytic reaction, indicating that the Pd species is still divalent after allylation. As shown in Table 2, the XPS signal of $Pd_{3d5/2}$ also supports the presence of Pd(II) after the reaction. These results indicate that the robust structure of the Pd complex is stabilized by the bisphosphine ligand, inhibiting the aggregation of Pd(0) particles during the catalytic reaction.

On the other hand, the Pd-catalyzed allylation is widely accepted to proceed via the formation of π-allylpalladium(II) and a Pd(0) species. For promoting the allylation, such active Pd species should be form from the PP-Pd(η^1-allyl)Cl structure on the SiO_2 surface. As shown in Table 2 and Figure 2(C), the XPS signal position of Cl_{2p} shifted from 198.0 eV to 199.8 eV after the catalytic reaction, suggesting the formation of potassium chloride.[12] The curve-fitting analysis of EXAFS spectra also indicates the decrease of the Pd-P/Cl coordination number (N) of SiO_2/DABCO/PP-Pd from 3.0 to 2.2 after the catalytic reaction (Table 3). These results are indicative of the removal of Cl from the PP-Pd(η^1-allyl)Cl complex. The reaction of SiO_2/DABCO/PP-Pd with ethyl acetoacetate and K_2CO_3 without allylmethylcarbonate afforded a small amount of the allylated product. On the other hand, XPS and EXAFS curve-fitting analysis results barely changed after the treatment of SiO_2/DABCO/PP-Pd with only allylmethylcarbonate (SiO_2/DABCO/PP-Pd-treated, Table 2 and 3). These results

View Article Online
DOI: 10.1039/C6CY00593D

indicate that the surface PP-Pd(η^1-allyl)Cl complex first reacts with the nucleophile, affording the allylated nucleophile, KCl, and monomeric Pd(0) (Scheme 5). Second, the monomeric Pd(0) species immediately reacts with allylmethylcarbonate to afford π-allylpalladium(II). The DABCO functionality immobilized on the SiO_2 surface, which is in close proximity to the PP-Pd complex, activates the nucleophile, followed by the reaction between the activated nucleophile and π-allylpalladium(II) to form the allylated product.

View Article Online
DOI: 10.1039/C6CY00593D

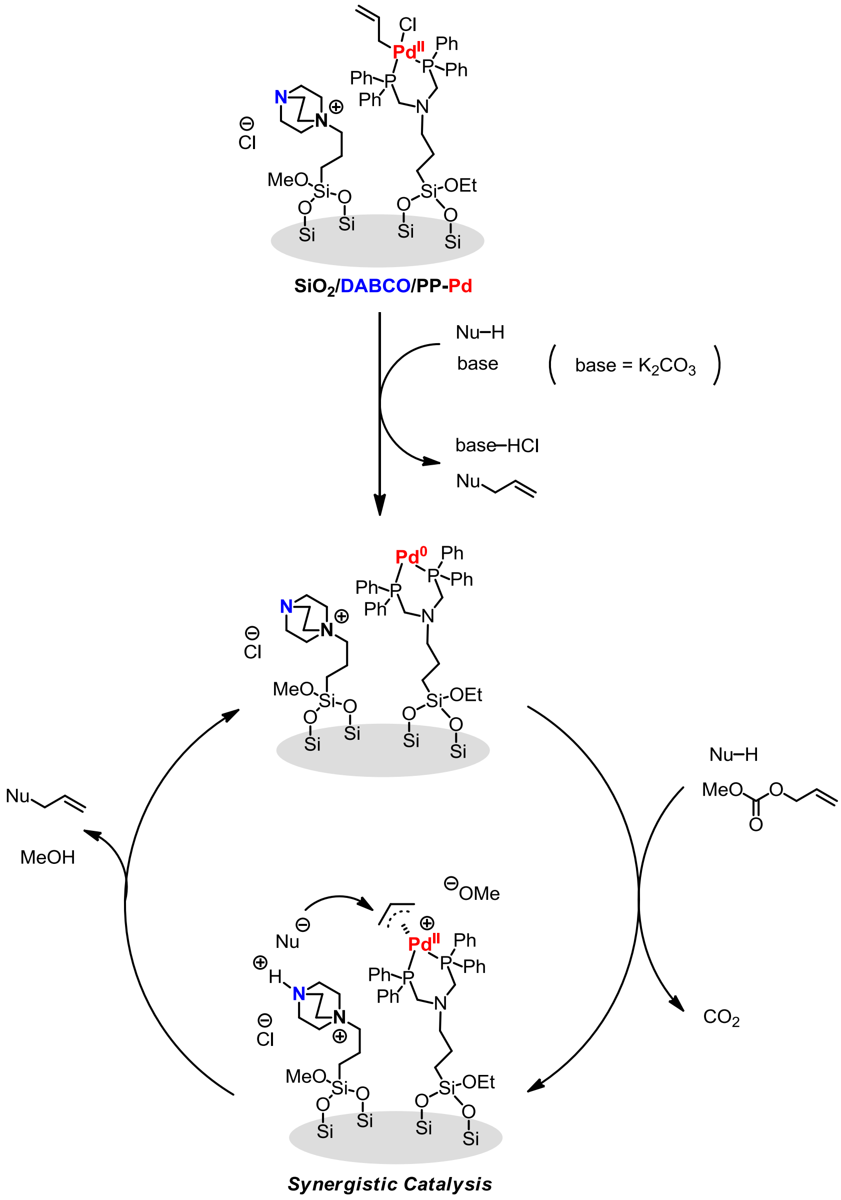

Scheme 5. Proposed catalyst activation and catalytic reaction mechanism using SiO$_2$/DABCO/PP-Pd

Conclusion

In this study, Pd-bisphosphine complex and several organic functionalities immobilized on the same SiO$_2$ surface were characterized in detail by solid-state NMR, XPS, and XAFS. The results obtained from the curve-fitting analysis of Pd K-edge

View Article Online
DOI: 10.1039/C6CY00593D

EXAFS spectra indicate that the Debye-Waller factor increases with increasing size of co-immobilized organic functions, suggesting that the immobilized functionalities are in close proximity with the Pd-bisphosphine complex. The Pd complex and DABCO functionality immobilized on the same SiO_2 surface synergistically catalyzed the allylation reaction: a TON of up to 106000 was achieved. EXAFS study of the used catalyst indicated that the reaction proceeds via the formation of π-allylpalladium(II) and a monomeric Pd(0) species. Synergism between immobilization methods for well-defined molecules on solid surfaces and atomic-level characterization techniques for these functionalized surfaces provides new opportunities for the creation of highly efficient heterogeneous catalysts.

Acknowledgements

We thank Dr. Yohei Uemura (Institute for Molecular Science) for his support with XAFS analysis. This study was conducted under the approval of the SAGA-LS Advisory Committee (Proposal No. 1504037F). This study was supported by JSPS KAKENHI (grant Nos. 25630362 and 15H04182) and JSPS Grant-in-Aid for Scientific Research on Innovative Areas “3D Active-Site Science” (grant No. 26105003). H.N. thanks Grant-in-Aid for JSPS Fellows (grant No. 26•12038).

References

[1] Pd catalysts for the allylation of nucleophiles (the Tsuji-Trost reaction): a) J. Tsuji, H. Takahashi, M. Morikawa, *Tetrahedron Lett.* **1965**, *6*, 4387; b) B. M. Trost, T. J. Fullerton, *J. Am. Chem. Soc.* **1973**, *95*, 292; c) B. M. Trost, D. L. Van Vranken, *Chem. Rev.* **1996**, *96*, 395; d) J. Tsuji, *Transition Metal Reagents and Catalysts*, Wiley: New

View Article Online
DOI: 10.1039/C6CY00593D

York, **2000**; e) J. Tsuji, *Palladium Reagents and Catalysts*, Wiley: Chichester, **2004**; f) B. M. Trost, *J. Org. Chem.* **2004**, *69*, 5813; g) B. M. Trost, *Org. Process Res. Dev.* **2012**, *16*, 185, and references therein.

[2] Homogeneous Pd catalysts for allylation; for examples, see: a) G. Hamasaka, F. Sakurai, Y. Uozumi *Chem. Commun.* **2015**, *51*, 3886; b) D. Laurenti, M. Feuerstein, G. Pèpe, H. Doucet, M. Santelli *J. Org. Chem.* **2001**, *66*, 1633. For a review of allylic amination, see: c) J.-C. Hierso, M. Beaupérin, P. Meunier *Eur. J. Inorg. Chem.* **2007**, 3767.

[3] Heterogeneous Pd catalysts for allylation: a) Y. M. A. Yamada, S. M. Sarkar, Y. Uozumi *J. Am. Chem. Soc.* **2012**, *134*, 3190; b) B. M. Trost, E. Keinan, *J. Am. Chem. Soc.* **1978**, *100*, 7779; c) J. Muzart, J.-P. Genet, A. Denis, *J. Organomet. Chem.* **1987**, *326*, C23; d) D. E. Bergbreiter, D. A. Weatherford, *J. Org. Chem.* **1989**, *54*, 2726; e) Y. Uozumi, H. Danjo, T. Hayashi *Tetrahedron Lett.* **1998**, *39*, 8303; f) H. Danjo, D. Tanaka, T. Hayashi, Y. Uozumi *Tetrahedron* **1999**, *55*, 14341; g) Y. Uozumi, K. Shibatomi *J. Am. Chem. Soc.* **2001**, *123*, 2919; h) K. H. Park, S. U. Son, Y. K. Chung, *Org. Lett.* **2002**, *4*, 4361; i) R. Akiyama, S. Kobayashi, *J. Am. Chem. Soc.* **2003**, *125*, 3412; j) F.-X. Felpin, Y. Landais *J. Org. Chem.* **2005**, *70*, 6441; k) Y. Uozumi, T. Suzuka *J. Org. Chem.* **2006**, *71*, 8644; l) T. Mitsudome, K. Nose, K. Mori, T. Mizugaki, K. Ebitani, K. Jitsukawa, K. Kaneda, *Angew. Chem.* **2007**, *119*, 3352; *Angew. Chem. Int. Ed.* **2007**, *46*, 3288; m) B. C. Ranu, K. Chattopadhyay, L. Adak, *Org. Lett.* **2007**, *9*, 4595; n) Y. Masuyama, Y. Nakajima, J. Okabe *Appl. Catal. A General* **2010**, *387*, 107; o) M. Lamblin, L. Nassar-Hardy, J.-C. Hierso, E. Fouquet, F.-X. Felpin, *Adv. Synth. Catal.* **2010**, *352*, 33; p) A. T. Dickschat, F. Behrends, S. Surmiak, M. Weiβ, H. Eckert, A. Studer, *Chem. Commun.* **2013**, *49*, 2195; q) Q. Zhao, Y. Zhu, Z. Sun, Y. Li, G. Zhang, F. Zhang, X. Fan,

View Article Online
DOI: 10.1039/C6CY00593D

J. Mater. Chem. A **2015**, *3*, 2609; r) J. Liu, X. Huo, T. Li, Z. Yang, P. Xi, Z. Wang, B. Wang, *Chem. Eur. J.* **2014**, *20*, 1154.

[4] For review of synergistic catalysis of metal complex and base, see: A. E. Allen, D. W. C. MacMillan, *Chem. Sci.* **2012**, *3*, 633.

[5] a) H. Noda, K. Motokura, A. Miyaji, T. Baba, *Angew. Chem.* **2012**, *124*, 8141; *Angew. Chem., Int. Ed.* **2012**, *51*, 8017; b) H. Noda, K. Motokura, A. Miyaji, T. Baba, *Adv. Synth. Catal.* **2013**, *355*, 973; c) K. Motokura, K. Saitoh, H. Noda, Y. Uemura, W.-J. Chun, A. Miyaji, S. Yamaguchi, T. Baba, *ChemCatChem* **2016**, *8*, 331.

[6] Rh complex-organic base bifunctional catalyst, see: H. Noda, K. Motokura, W.-J. Chun, A. Miyaji, S. Yamaguchi, T. Baba, *Catal. Sci. Technol.* **2015**, *5*, 2714.

[7] For SiO_2-supported Pd-bisphosphine complexes, see: M. Cai, J. Sha, Q. Xu, *J. Mol. Catal. A. Chemical* **2007**, *268*, 82.

[8] S.-D. Lee, B.-M. Kim, D.-W. Kim, M.-I. Kim, K. R. Roshan, M.-K. Kim, Y.-S. Won, D.-W. Park, *Appl. Catal. A General* **2014**, *486*, 69.

[9] XAFS results of SiO_2/PP-Pd and SiO_2/DABCO/PP-Pd were reported previously;[5c] however, these spectra are also shown in Supporting Information for comparison (Figure S5-S7).

[10] R. S. Corrêa, A. E. Graminha, J. Ellena, A. A. Batista, *Acta Crystallogr. Sect. C* **2011**, *67*, m304.

[11] E. Clot, O. Eisenstein, T.-C. Weng, J. Penner-Hahn, K. G. Caulton *J. Am. Chem. Soc.* **2004**, *126*, 9079.

[12] J. Stoch, M. Ladecka, *Appl. Sur. Sci.* **1988**, *31*, 426

View Article Online
DOI: 10.1039/C6CY00593D

Table 1. Elemental analysis of SiO_2-supported materials[a]

sample	C (mmol g^{-1})	N (mmol g^{-1})	Cl (mmol g^{-1})	Pd (mmol g^{-1})
SiO_2/Cl	3.8	-	0.8	-
SiO_2/DABCO	6.2	1.4	0.6	-
SiO_2/PP-Pd	11.9	0.4	0.3	0.28
SiO_2/DABCO/PP-Pd	11.5	1.1	0.7	0.17
SiO_2/Me/PP-Pd	9.6	0.3	0.3	0.18
SiO_2/Hex/PP-Pd	10.8	0.3	0.3	0.25

[a] Part of the data in this table were previously reported in ref.[5c]

View Article Online
DOI: 10.1039/C6CY00593D

Table 2. XPS analysis of SiO_2-supported Pd catalysts

Sample	binding energy (eV)			
	Pd $_{3d5/2}$	P $_{2p}$	N $_{1s}$	Cl $_{2p}$
SiO_2/PP-Pd	337.5	131.4	399.6	197.9
SiO_2/DABCO/PP-Pd	337.2	131.6	399.6, 402	198.0
SiO_2/Me/PP-Pd	337.2	131.1	399.2	197.6
SiO_2/Hex/PP-Pd	337.4	131.2	399.6	198.0
SiO_2/DABCO/PP-Pd-used	337.5	131.6	399.9, 402	199.8
SiO_2/DABCO/PP-Pd-treated[a]	337.4	131.6	399.6, 402	198.7
$PdCl_2$ [b]	338.1	-	-	199.2
KCl [c]	-	-	-	199.2

Reference: Si 2p (103.4 eV).

[a] SiO_2/DABCO/PP-Pd catalyst treated with allylmethylcarbonate.

[b] Data from ref. [7]

[c] Data from ref. [12]

View Article Online
DOI: 10.1039/C6CY00593D

Table 3. Curve-fitting analysis of EXAFS spectra for SiO_2-supported PP-Pd complex catalysts[a]

Sample	shell	N [b]	r [c] (Å)	$\Delta\sigma^2$ [d] (Å^2×10^{-3})	ΔE [e] (eV)	Rf [f] (%)
SiO_2/PP-Pd	Pd-P/Cl	2.6	2.26	2.80	–2.07	1.95
		±0.4	±0.01	±0.20	±2.03	
SiO_2/DABCO/PP-Pd	Pd-P/Cl	3.0	2.26	5.05	–0.61	3.05
		±0.5	±0.01	±0.20	±1.98	
SiO_2/Me/PP-Pd	Pd-P/Cl	2.6	2.27	3.63	–6.81	1.28
		±0.4	±0.01	±0.20	±2.09	
SiO_2/Hex/PP-Pd	Pd-P/Cl	2.9	2.27	4.86	–3.11	2.87
		±0.4	±0.01	±0.20	±2.00	
PP-Pd (THF solution) [g]	Pd-P/Cl	3.0	2.29	2.64	–5.89	1.28
		(fix)	±0.01	±0.03	±1.91	
SiO_2/DABCO/PP-Pd-used	Pd-P/Cl	2.2	2.25	4.86	–8.75	2.15
		±0.3	±0.01	±0.20	±2.17	
SiO_2/DABCO/PP-Pd-treated [h]	Pd-P/Cl	2.7	2.26	5.62	–4.71	2.28
		±0.4	±0.01	±0.20	±2.04	
$Pd(II)Cl_2(PPh_3)_2$ [i]	(Pd-P)	2	2.34 [j]			
	(Pd-Cl)	2	2.30 [j]			

[a] Fourier transform and Fourier-filtering region were limited, where Δk = 2.8 ~ 15 Å^{-1}. and Δr = 1.4 ~ 2.2 Å, respectively.

[b] Coordination number.

[c] Bond distance between absorber and backscatter atoms.

[d] The Debye-Waller factor (DW), which is relative to the DW of the reference.

[e] The inner potential correction accounts for the difference in the inner potential between the sample and reference

[f] A goodness of curve fit.

[g] Homogeneous THF solution of the PP-Pd complex.

[h] SiO_2/DABCO/PP-Pd catalyst treated with allylmethylcarbonate.

[i] Data from ref. [10]

[j] Average value was reported.

DOI: 10.1039/C6CY00593D

Table 4. The allylation catalyzed by SiO_2-supported Pd complexes [a]

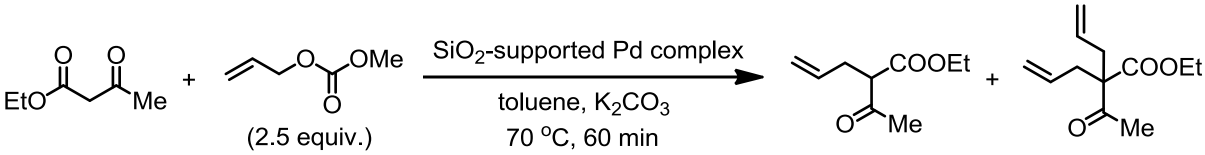

entry	catalyst	conversion (%)	yield (mono/di) (%)	TON ($\times10^2$)[b]
1	SiO_2/DABCO/PP-Pd	>99	18 / 81	3.0
2	SiO_2/PP-Pd	98	40 / 49	2.3
3	SiO_2/Me/PP-Pd	83	62 / 21	1.7
4	SiO_2/Hex/PP-Pd	90	55 / 31	2.0
5	PP-Pd	97	48 / 42	2.2
6 [c]	PP-Pd + DABCO	83	53 / 22	1.6

[a] Reaction conditions: ethyl acetoacetate (0.50 mmol), allylmethylcarbonate (1.25 mmol), Pd catalyst (Pd: 3.0 μmol), K_2CO_3 (0.25 mmol), toluene (2 mL), 70 °C, 60 min.

[b] TON was calculated as follows: TON = (moles of nucleophile)×[(yield of the mono-product) + 2×(yield of the di-product)] / (moles of Pd).

[c] 6μmol of DABCO was added.

View Article Online
DOI: 10.1039/C6CY00593D

Table 5. The allylation catalyzed by SiO_2/DABCO/PP-Pd under solvent-free conditions[a]

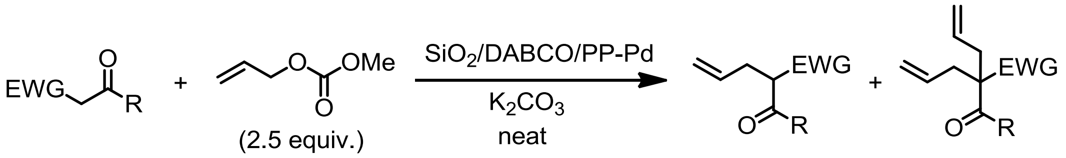

entry	nucleophile	(mmol)	Pd (μmol)	K_2CO_3 (mmol)	Time (h)	Yield (mono/di) (%)	TON [b]
1 [c]	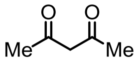	12.6	0.21	0.025	216	3 / 87	106000
2	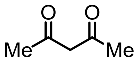	9.0	1.5	0.13	31	<1 / >99	12000
3	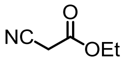	9.0	1.5	0.13	5	<1 / 93	11200
4	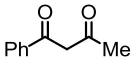	9.0	1.5	0.13	48	<1 / 98	11800
5	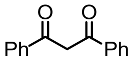	9.0	1.5	0.13	54	83 / 12	6400
6	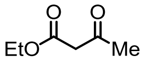	9.0	1.5	0.13	24	<1 / 98	11700
7 [d]	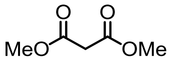	9.0	1.5	0.13	31	<1 / 95	11400
8	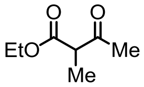	18.0	1.5	0.13	113	98 / -	11700
9	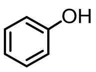	18.0	1.5	0.13	124	84 / -	10100

[a] Reaction conditions: nucleophile, allylmethylcarbonate (2.5 equiv.), K_2CO_3, SiO_2/DABCO/PP-Pd, 70 °C, neat. Yield was determined by ^1H NMR analysis using an internal standard. [b] TON was calculated as follows: TON = (moles of nucleophile)×[(yield of the mono-product) + 2×(yield of the di-product)] / (moles of Pd). [c] 80 °C. [d] 100 °C.

View Article Online
DOI: 10.1039/C6CY00593D

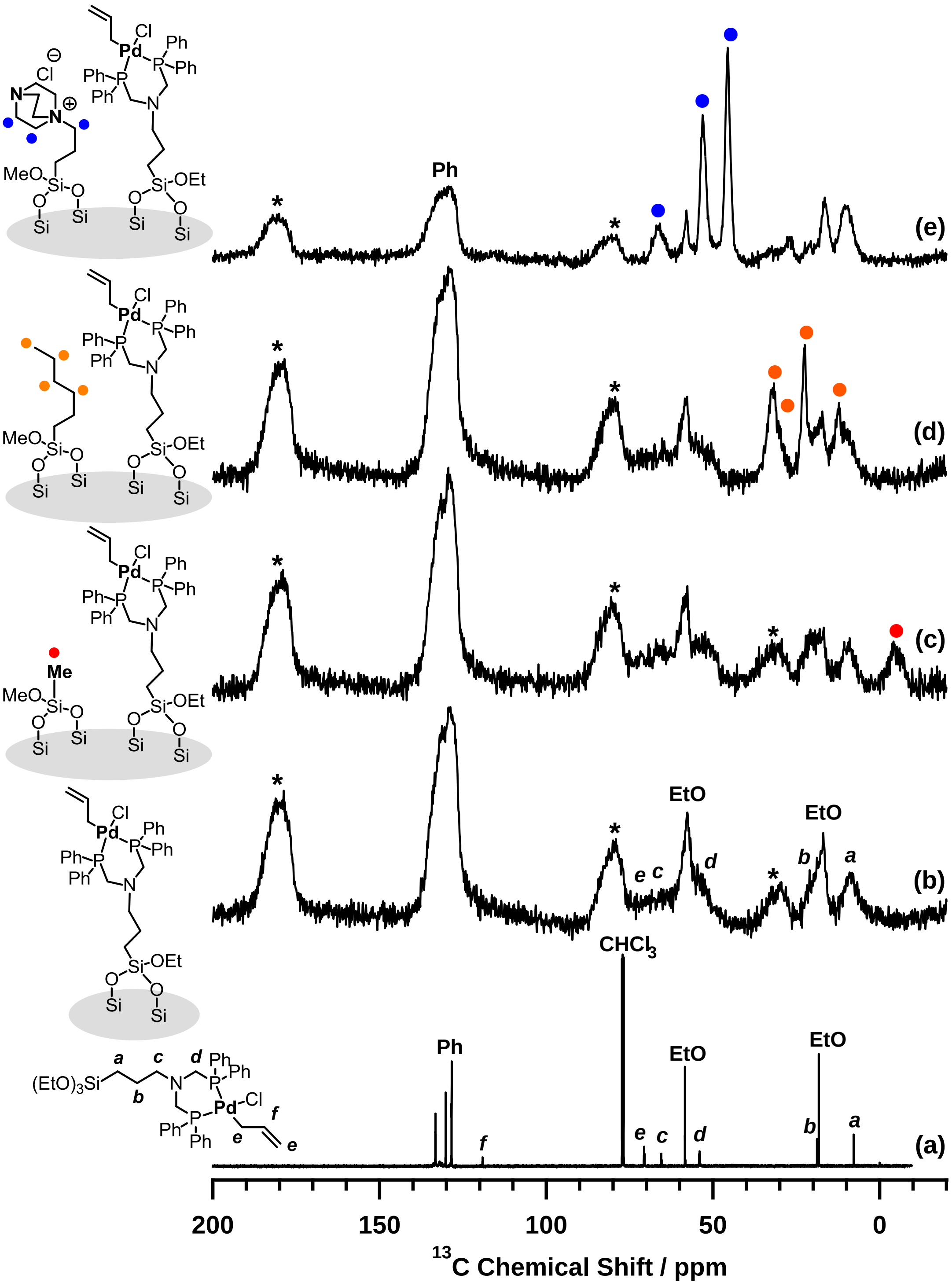

Figure 1. ^{13}C NMR spectra of (a) $CDCl_3$ solution of PP-Pd, (b) SiO_2/PP-Pd,[5c] (c) SiO_2/Me/PP-Pd, (d) SiO_2/Hex/PP-Pd, and (e) SiO_2/DABCO/PP-Pd.[5c] ^{13}C CP/MAS NMR was conducted for SiO_2-supported materials. (*) indicate spinning side bands.

View Article Online
DOI: 10.1039/C6CY00593D

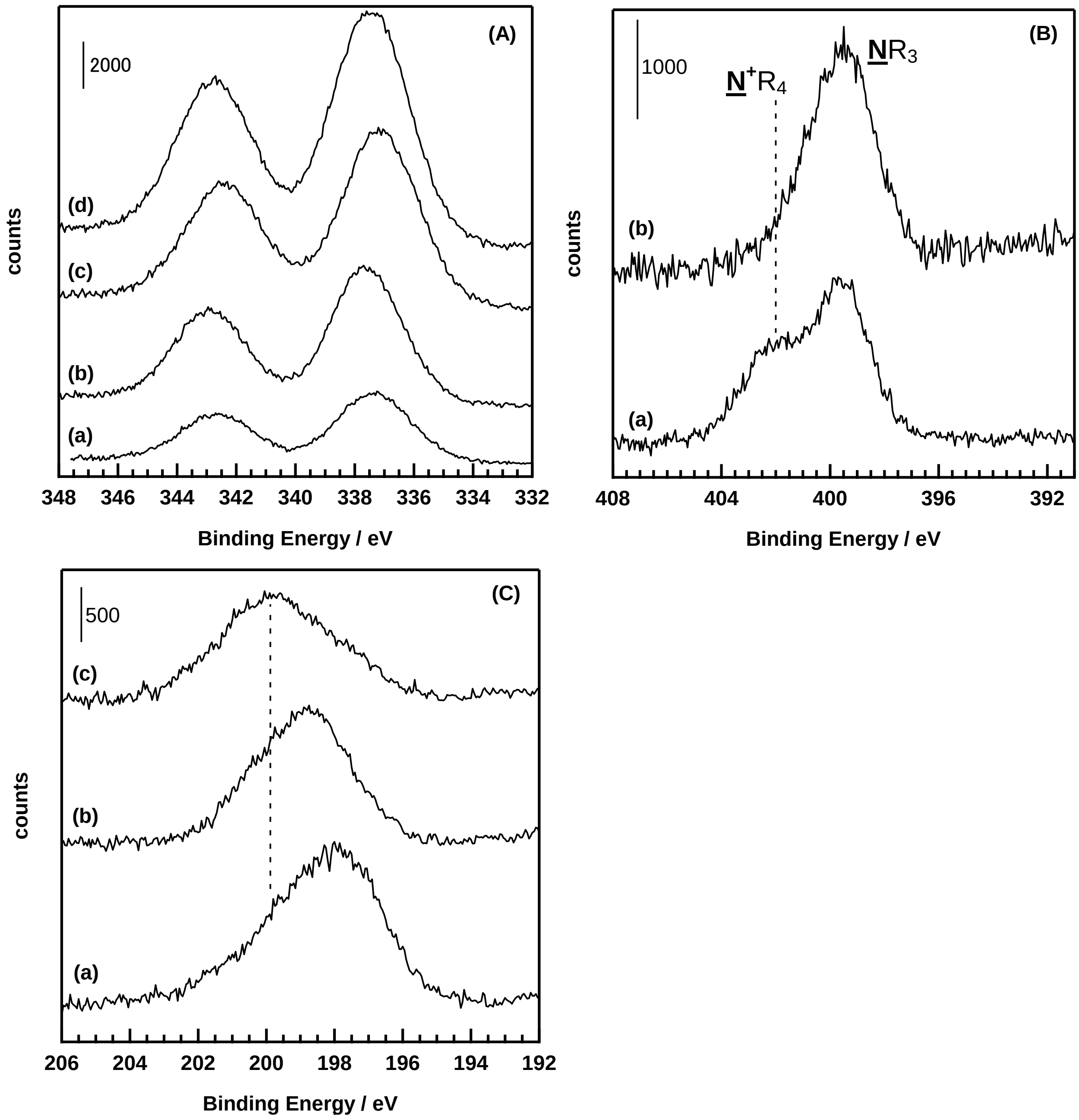

Figure 2. XPS spectra of **(A)** Pd 3d of (a) SiO_2/DABCO/PP-Pd, (b) SiO_2/PP-Pd, (c) SiO_2/Me/PP-Pd, and (d) SiO_2/Hex/PP-Pd, **(B)** N 1s of (a) SiO_2/DABCO/PP-Pd and (b) SiO_2/PP-Pd, and **(C)** Cl 2p of (a) SiO_2/DABCO/PP-Pd, (b) SiO_2/DABCO/PP-Pd-treated, and (c) SiO_2/DABCO/PP-Pd-used.

View Article Online
DOI: 10.1039/C6CY00593D

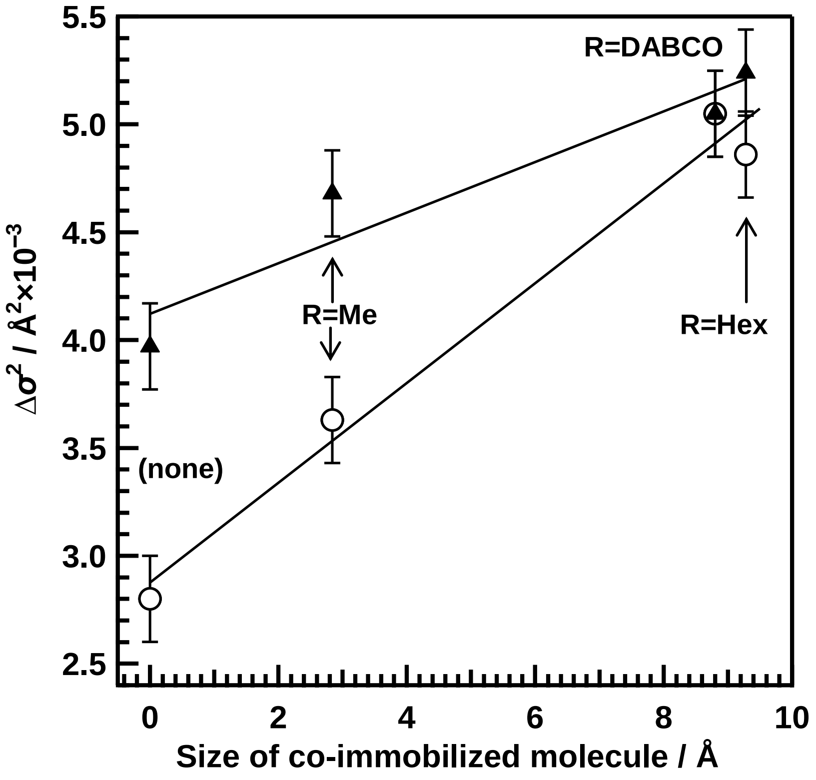

Figure 3. Debye-Waller factor ($\Delta\sigma^2$) of k^3-weighted Pd K-edge EXAFS spectra of SiO_2-supported Pd complexes (SiO_2/**R**/PP-Pd) plotted against the size of the co-immobilized molecule on the same SiO_2 surface (○). The $\Delta\sigma^2$ values determined by the simulation with a fixed coordination number value (N=3) are also shown (▲). Size of the co-immobilized molecule is the distance between oxygen and the edge atom of the silane coupling reagents, which have quaternized DABCO, *n*-hexyl, and methyl groups.

View Article Online
DOI: 10.1039/C6CY00593D

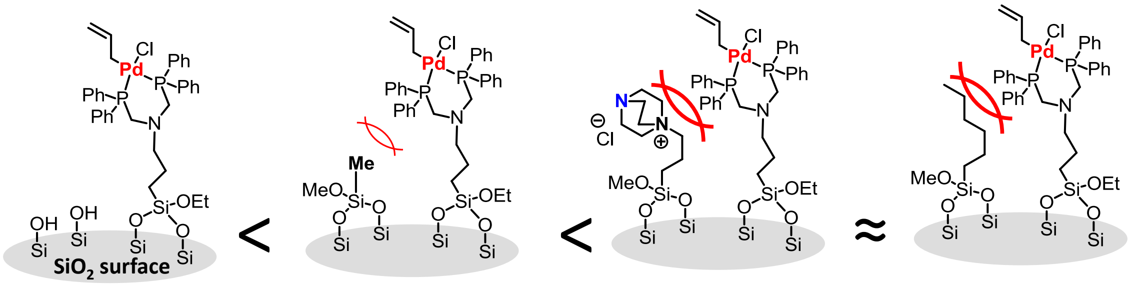

Figure 4. Order of the steric effect around immobilized Pd-bisphoshine complexes estimated from their Debye-Waller factors ($\Delta\sigma^2$) of k^3-weighted Pd K-edge EXAFS spectra.

View Article Online
DOI: 10.1039/C6CY00593D

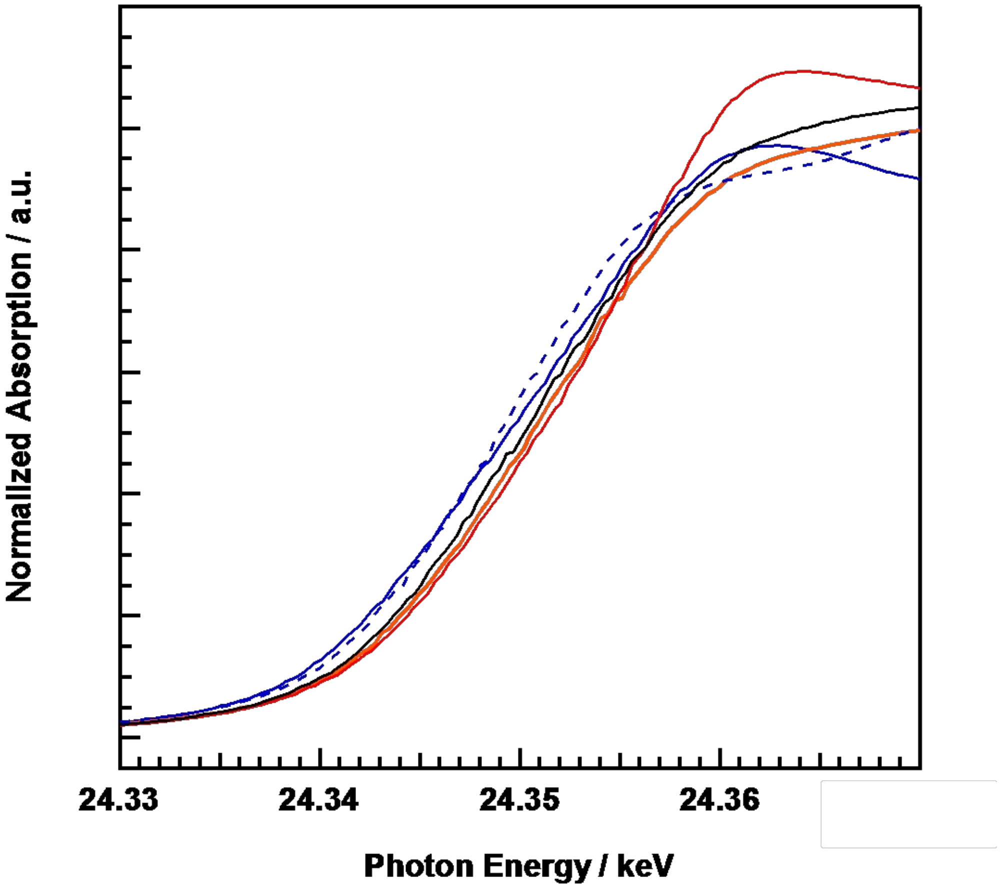

Figure 5. Pd K-edge XANES spectra of $Pd^{II}O$ (red line), SiO_2/DABCO/PP-Pd (bold orange line), SiO_2/DABCO/PP-Pd-used (black solid line), Pd^0 foil (blue solid line), and $Pd^0(PPh_3)_4$ (blue dash line).

View Article Online
DOI: 10.1039/C6CY00593D

Graphical Abstract